Volume 15
Number 19
21 May 2024
Pages 6981–7360

Chemical Science

rsc.li/chemical-science

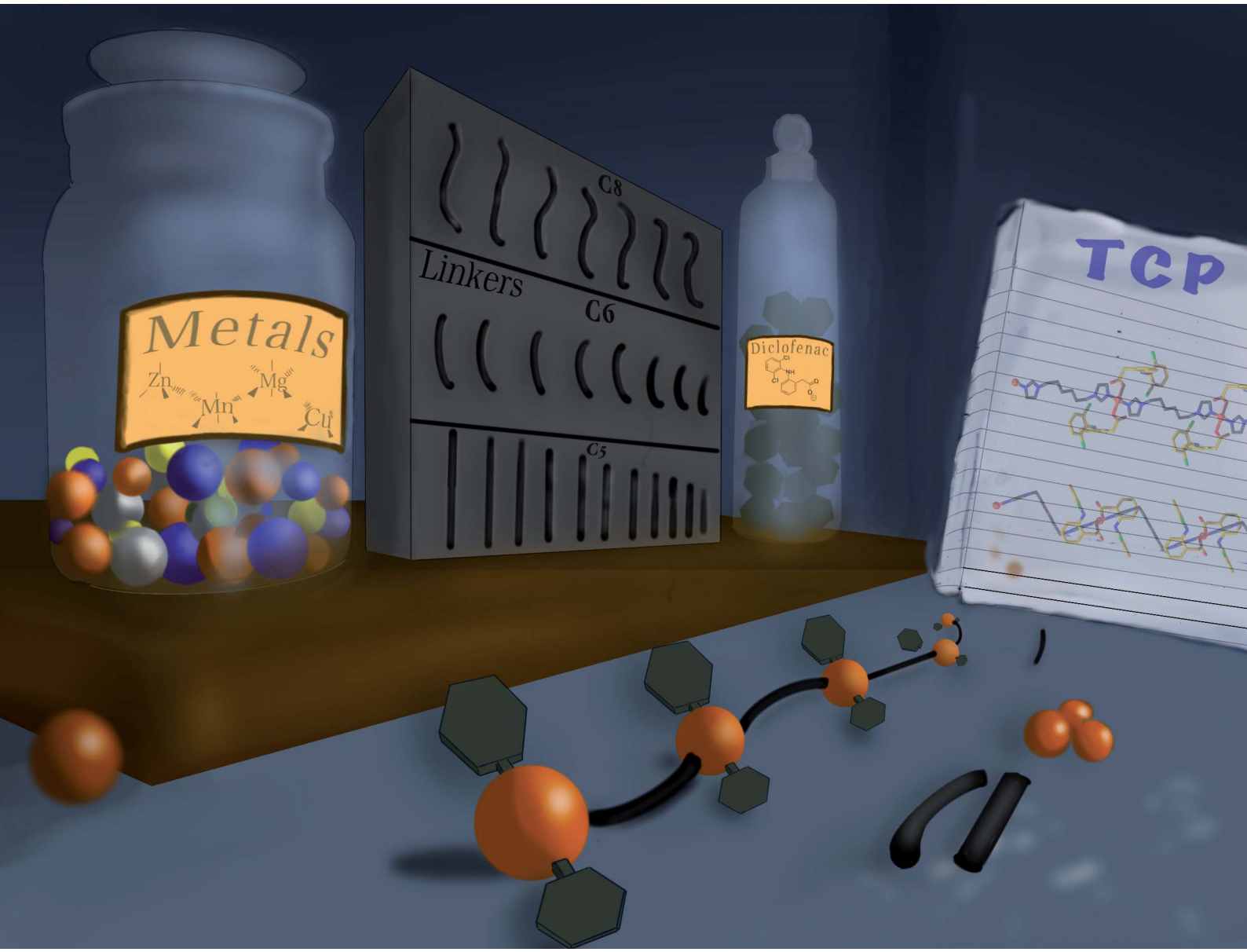

ISSN 2041-6539

ROYAL SOCIETY OF CHEMISTRY

EDGE ARTICLE

V. Nicholas Vukotic *et al.*

Therapeutic coordination polymers: tailoring drug release through metal–ligand interactions

Chemical Science

ROYAL SOCIETY OF CHEMISTRY

EDGE ARTICLE

View Article Online
View Journal | View Issue

Cite this: *Chem. Sci.*, 2024, **15**, 7041

All publication charges for this article have been paid for by the Royal Society of Chemistry

Received 30th January 2024
Accepted 10th April 2024

DOI: 10.1039/d4sc00732h

rsc.li/chemical-science

Therapeutic coordination polymers: tailoring drug release through metal–ligand interactions†

Jennifer N. Murphy,[ab] Joy-Lynn Kobti,[a] Michelle Dao,[a] Darcy Wear,[acd] Michael Okoko,[a] Siyaram Pandey[a] and V. Nicholas Vukotic *[a]

Developing tunable materials which exhibit sustained drug release is a considerable challenge. Herein, we report the concept of Therapeutic Coordination Polymers (TCPs); non-porous coordination polymers constructed from biocompatible components which demonstrate tunable zero-order drug release kinetics upon degradation of metal–ligand bonds. TCPs were constructed from three principal components: (i) a cationic metal center (M = Mg^{2+}, Mn^{2+}, Zn^{2+}, or Cu^{2+}); (ii) an anionic drug (Diclofenac); and (iii) an alkyl bis-imidazole organic ligand which behaves as a "linker" between metal centers. Most drug-release materials, such as amorphous polymer dispersions, or metal–organic frameworks rely on a diffusion-based mechanism for drug release, but the degradation-controlled release of drugs from non-porous one-periodic coordination polymers has been largely unexplored. TCPs described herein exhibit a high wt% of pharmaceutical (>62%), tailorable zero-order drug release rate kinetics which span over three orders of magnitude, and stimuli-responsive drug release behavior making them well suited for extended drug-release applications.

Introduction

Controlled and sustained drug-release materials can be used to develop better medical treatments by improving a pharmaceutical's inherent physiochemical properties (*e.g.*, solubility and bioavailability) to maximize the drug's therapeutic benefit.[1,2] These materials are particularly advantageous in cases where drugs have a narrow therapeutic index, fast clearance time, or short elimination half-life, which often leads to the need for higher and more frequent dosages to maintain the therapeutic effect.[3] Considering that the development of a single new pharmaceutical takes considerable time and resources (estimated cost of USD 2.6 billion, in 2020),[4] the ability to improve the performance of existing drugs has significant advantages.[5,6]

Commonly used drug-release materials include excipients, such as cellulose used in solid-state formulations,[7,8] amorphous organic polymer dispersions,[9,10] lipids,[11] ceramics (*e.g.*, hydroxyapatite), and, most recently, porous materials, such as porous coordination polymers (PCPs)[12] and metal–organic frameworks (MOFs).[13–17] The barriers associated with developing ideal drug-release materials are complex and change depending on the target drug and route of administration (*e.g.*, oral, intravenous, subcutaneous, transdermal, or ocular).[2] Thus, creating materials which consistently incorporate the desired amount of a therapeutic and control the drug's release rate is still a considerable challenge.

Many drug-release materials, ranging from amorphous polymer dispersions to metal–organic frameworks, suffer the same fundamental issue: drug uptake and release is primarily accomplished through a diffusion-based mechanism.[18] Unfortunately, reliance on drug loading and release by diffusion often results in poor control over drug release kinetics and can lead to 'burst release'. In this case, the drug is rapidly dispersed into the surrounding media, often overshooting the therapeutic dosage and potentially reaching toxic dosage concentrations.[6] Indeed, it has been over 20 years since Langer & Peppas reported that a surface erosion mechanism caused by the degradation of a material (*e.g.*, polyanhydride-based polymers) offers far superior control, compared to diffusion-based release.[19] Unfortunately, it is very difficult to accomplish degradation-based drug release with organic polymers, which possess other significant drawbacks, including low wt% drug loadings and reproducibility issues.[18,20–23] Although solid-state forms (*e.g.*, polymorphs, salts, and co-crystals) in which the drug is incorporated in a stoichiometric ratio exhibit consistent drug incorporation, high wt%, and degradation-based drug release,[24] these solid-state forms are held together with relatively weak

[a]*Department of Chemistry and Biochemistry, University of Windsor, 401 Sunset Avenue, Windsor, ON N9B 3P4, Canada. E-mail: nick.vukotic@uwindsor.ca*

[b]*Department of Chemistry, University of Guelph, 50 Stone Rd E, Guelph, ON N1G 2W1, Canada*

[c]*Department of Pharmacology and Toxicology, University of Toronto, Toronto, ON M5R 0A3, Canada*

[d]*Brain Health Imaging Centre, Centre for Addiction and Mental Health, Toronto, ON M5T 1R8, Canada*

† Electronic supplementary information (ESI) available. CCDC 2237924–2237934. For ESI and crystallographic data in CIF or other electronic format see DOI: https://doi.org/10.1039/d4sc00732h

non-covalent interactions and suffer from a limited ability to tune drug release rates.[24,25] In consideration of these factors, and in contrast to the vast majority of known drug release materials, we have developed the concept of Therapeutic Coordination Polymers (TCPs), non-porous coordination polymers which utilize metal–ligand interactions to achieve degradation-based drug release.

TCPs described herein were constructed from a combination of three principal components: (i) a cationic metal center (**M** = Mg^{2+}, Mn^{2+}, Zn^{2+}, or Cu^{2+}); (ii) an anionic non-steroidal anti-inflammatory drug (NSAID), such as Diclofenac (**Diclo**); and (iii) an alkyl bis-imidazole bidentate ligand which behaves as a biocompatible "linker" between metal centers (**biim-X** where X = 5, 6, or 8, CH_2 linking units between terminal imidazoles). The general formula of the smallest repeating unit within a linear TCP is **M(Diclo)$_2$(biim-X)**, abbreviated **MDicloX** (Scheme 1).

Our lab has demonstrated that TCPs can be formed from several anionic NSAIDs containing carboxylate groups.[26] Diclofenac (2-(2,6-dicholoroanilino)phenylacetate) proved to be an ideal target for our initial drug release investigations, due to its size, solubility, photophysical properties,[27] and ease of incorporation. Diclofenac is used as an anti-inflammatory, analgesic, and antipyretic drug to treat pain, rheumatic inflammations, and osteoarthritis. The acid form is known to have poor solubility, which can be drastically improved by utilizing the sodium salt of the drug.[28] Despite this, numerous daily doses are typically required to maintain its therapeutic effect, which could be dramatically improved by a controlled or sustained-release oral formulation or drug-release implant.[29,30]

While coordination polymers, such as infinite coordination polymers (ICPs), have been previously investigated as drug release materials, studies which focus on direct coordination of the pharmaceutical to the CP are rare, and mainly involved poorly water-soluble pyridine-based linkers which resulted in insoluble by-products upon exposure to aqueous dissolution media and incomplete release of their drug payload.[31–34] To the best of our knowledge, the imidazole-based TCPs described herein are the first drug-containing coordination polymers to behave as tunable drug release 'matrix' materials, exhibiting complete, consistent, and tunable drug release rates. This has allowed us to determine, for the first time, the specific intrinsic dissolution rate (*i.e.*, degradation rate) for a series of drug-containing coordination polymers which have been pressed into monoliths. These results represent a significant breakthrough in the search for tunable sustained drug release materials and a new approach to utilizing non-porous coordination polymers with direct incorporation of pharmaceuticals, rather than suffering from the poor control over diffusion which plagues porous materials (*e.g.* organic polymers and MOFs).[35]

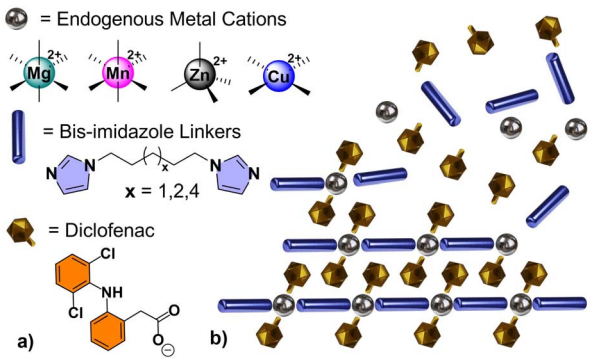

Scheme 1 (a) Components of TCPs (MDicloX): M = Mg^{2+}, Mn^{2+}, Zn^{2+}, or Cu^{2+} metal cations, Diclo = diclofenac anions, and X = bis-imidazole linkers with total carbon chain lengths 5, 6, or 8 between imidazoles, (b) representation of drug release from TCPs *via* degradation of metal–ligand interactions.

Results and discussion

Synthesis & characterization of TCPs

TCPs were synthesized by combining alcoholic solutions of their principal components (M^{2+} nitrate salt, biim-linker, and Diclofenac) at ambient temperatures. The ambient reaction conditions are particularly advantageous, as no hydrothermal or solvothermal synthesis was necessary which might result in unwanted decomposition of the pharmaceutical component (Diclofenac is known to undergo decomposition at elevated temperatures).[36] The bis-imidazole linkers are readily soluble in alcoholic and aqueous solutions, in comparison to highly conjugated ligands used in other studies which have hindered drug release from the resultant materials.[31,32] The bis-imidazole linkers are used in excess during the synthesis to function as a base to deprotonate the carboxylic acid of Diclofenac, forming the carboxylate derivative and initiating TCP formation. Single crystal structures of the TCPs are shown in Fig. 1 and Fig. S1–S11,† while a summary of crystallographic parameters is listed in Table S1.2.† All TCPs contain two Diclofenac anions coordinated to each metal center in a monotopic fashion and an imidazole-based linker which joins adjacent metal centers to form one-periodic coordination polymer strands (Fig. 1).

The coordination environment within each TCP depends on the geometric preference of the metal center; Mg^{2+} and Mn^{2+} TCPs adopt an octahedral geometry with coordinated solvent molecules (*e.g.*, EtOH), while Zn^{2+} TCPs have a distorted tetrahedral geometry with τ_4 parameters ranging from 0.83 to 0.93,[37] and Cu^{2+} TCPs exhibit a square planar geometry. For Mg^{2+}, Mn^{2+}, and Cu^{2+} TCPs, the biim linkers adopt a *trans* disposition while the angles between biim linkers for Zn^{2+} TCPs vary from 106 to 119° because of their tetrahedral geometry, forming one-periodic polymer strands which propagate in an undulating manner. The Diclofenac units in all TCPs undergo intramolecular H-bonding between the N–H group and the carbonyl O atom (Fig. S17†). The polymer strands contain a high weight percentage of the active pharmaceutical ingredient (61.7–68.6 wt%) and are densely packed to form non-porous crystalline solids. TCP strands organize in a parallel or orthogonal fashion in the solid-state, facilitated by intermolecular forces such as C–H···π interactions between aromatic moieties of the Diclofenac molecules in adjacent polymer strands (Fig. S12–S20†).

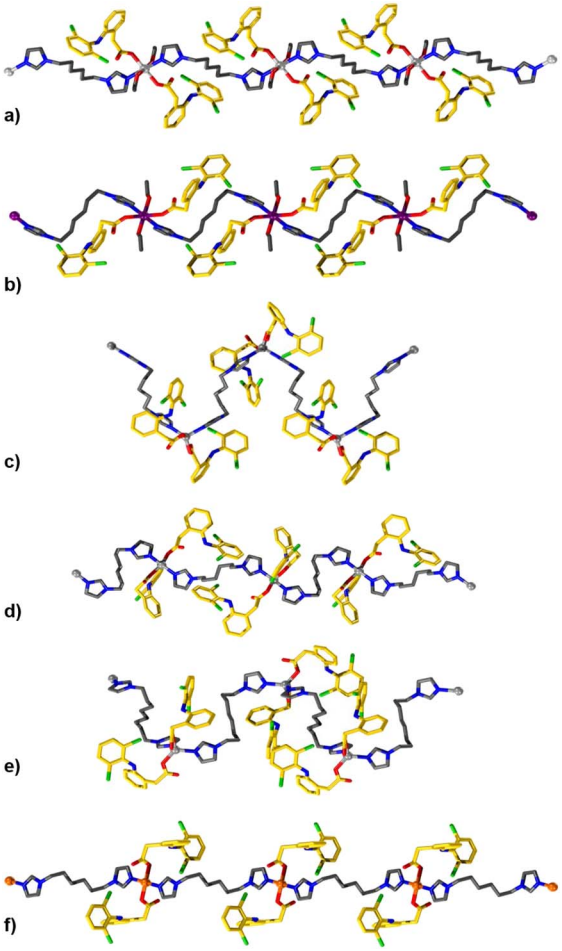

Fig. 1 Single-crystal structures of TCPs, (a) **MgDiclo6**, (b) **MnDiclo6**, (c) **ZnDiclo5**, (d) **ZnDiclo6**, (e) **ZnDiclo8**, and (f) **CuDiclo6**. Mg = light grey, Mn = purple, Zn = grey, Cu = orange, N = blue, O = red, Cl = green, bis-imidazole and diclofenac C-atoms are shown in silver and gold, respectively.

Typically, densely packed non-porous coordination polymers are not targeted as drug-release materials, as many systems (such as metal–organic frameworks)[38,39] rely on the porous structure of the material for diffusion-based drug uptake and release. However, for a degradation-based approach, densely packed coordination polymers are ideal, as the drugs are an integral part of the material, and the release rate can be tuned by altering the strength of the metal–ligand bonds and intermolecular forces within the TCP. At high concentrations (0.20 M), bulk quantities of TCPs can be obtained rapidly. At lower concentrations, as described in the experimental section, large single crystals of the TCPs form, see Fig. 2. In cases where the organic linker is kept constant between Diclofenac-containing TCPs, the formation time and degradation time strongly depend on the metal cation. For example, the relative speed of TCP formation (Mg^{2+} < Mn^{2+} < Zn^{2+} < Cu^{2+}) correlates with the increasing Lewis acidity of the metal ions and known formation constants of transition metals within the Irving-Williams series.[40,41] For Cu^{2+} specifically, crystallization was so rapid that it was possible to observe single crystal growth in real-time

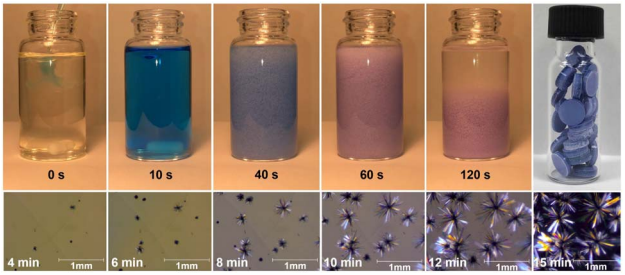

Fig. 2 Rapid synthesis of TCP **CuDiclo6** upon addition of $Cu(NO_3)_2$ in MeOH (top) with pressed monoliths depicted (top right) and formation of large single crystals at lower concentration in MeOH (bottom).

(video see ESI†). Fig. 2 depicts images from the bulk preparation of **CuDiclo6**, as well as those of single crystal growth obtained when the concentration of the solution was decreased to slow crystal formation. It is of interest to note that these crystal growth images also represent the formation of the coordination polymer itself, allowing one to directly observe the polymerization event leading to TCPs in real time. All TCP materials were characterized by Fourier transform infrared spectroscopy (Fig. S21–S31†), powder X-ray diffraction (Fig. S32–S49†), and scanning electron microscopy was used to image crystals of **CuDiclo6**, **ZnDiclo6**, **MgDiclo6**, and **MnDiclo6** TCPs (Fig. S82–S85†). The thermal stability of all TCPs was determined using thermogravimetric analysis. In the case of **CuDiclo6**, the structure contains interstitial MeOH, and the bulk powder was found to desolvate over time to a new dehydrated phase **CuDiclo6′** (Fig. S51†). All TCP materials exhibited decomposition at temperatures above 200 °C; Cu^{2+} TCPs showed thermal stability up to 200 °C, whereas all other TCPs decomposed above 250 °C (Fig. S50–S60†).[42] For TCPs containing solvent (coordinated or interstitial), there was clear evidence of mass loss due to the solvent release before polymer decomposition.

Drug release studies

To explore drug release rates from TCPs in a form that could be used as a medical implant or as an orally taken medication, solid cylindrical monoliths were produced. The anionic Diclofenac drug molecules within these monoliths can be thought of as being embedded within the cationic scaffold of the coordination polymer 'matrix'. Approximately 30 mg of each TCP was pressed into a 5 mm diameter cylindrical monolith by applying 2 tonnes of pressure for 60 s using a Carver hydraulic press. The top-right image in Fig. 2 depicts a photograph of a vial filled with monoliths of **CuDiclo6′**, demonstrating the ease with which TCP-based materials can be pelletized. To determine if compression during monolith formation altered the molecular structure of TCPs, powder X-ray diffraction (PXRD) patterns were collected on intact monoliths of **MgDiclo6**, **MnDiclo6**, **ZnDiclo6**, and **CuDiclo6′**. While collected reflections were broader due to the increased sample thickness of the pellets in transmission geometry, the pressure from monolith formation did not significantly alter the PXRD patterns of these materials (Fig. S46–S49†). In addition, the dissolution profile of **MgDiclo6**

did not exhibit any significant differences when pressed at 1 tonne in comparison to 2 tonnes (Fig. S69†), demonstrating that over this pressure range drug release was not pressure dependent.

Fig. 3a shows the drug release profile of Diclofenac from monoliths of TCPs formed using the same biim-6 linker with Mg^{2+}, Mn^{2+}, and Zn^{2+} metal ions. Monoliths were placed in stainless steel baskets for over 72 h while immersed in 0.05 M phosphate buffer (pH 6.8) at 37 °C with aliquots taken at specified time intervals and analyzed *via* UV-Vis spectroscopy (Fig. S61–S81†). A phosphate buffer system with a pH of 6.8 was chosen as a default buffer system, as it allowed for good comparison and separation of relative drug release rates from TCPs and not due to its ability to mimic any particular bodily fluid, which would require the addition of lipids, serum proteins, and other relevant biomolecules.[43] The substantial differences in the release of Diclofenac from these three TCPs demonstrate the significant effect the metal ion has on the release of Diclofenac from these materials. **MgDiclo6** degrades the most rapidly, with complete release of Diclofenac in ~8 h, while **MnDiclo6** releases completely after ~48 h, and **ZnDiclo6** degrades the slowest with <10% of Diclofenac released after ~72 h. The release of Diclofenac from **CuDiclo6′** was studied, however, the degradation rate proved to be too slow to be measured under these conditions.

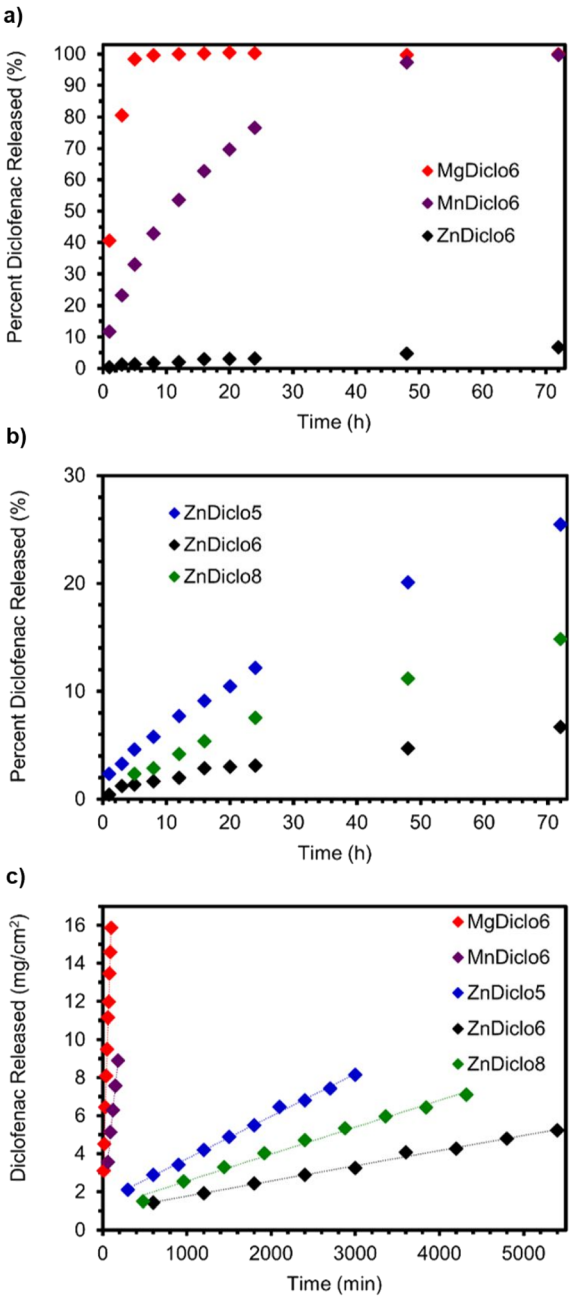

Fig. 3 Drug release profiles from 5 mm TCP monoliths in 0.05 M phosphate buffer, pH 6.8 at 37 °C. (a) **MgDiclo6** (red), **MnDiclo6** (purple), and **ZnDiclo6** (black) demonstrate effect of varying metal ion composition, (b) **ZnDiclo5** (blue), **ZnDiclo6** (black), and **ZnDiclo8** (green) demonstrate effect of varying linker composition, (c) intrinsic dissolution release (IDR) rates of Diclofenac from TCPs measured using a Woods apparatus, demonstrating prolonged zero-order release kinetics.

By keeping the metal ion constant, we were also able to investigate the effect linker length has on TCP degradation. A series of Zn^{2+} TCP monoliths containing biim-5, -6, and -8 linkers were exposed to the same degradation conditions as described above. Over a 72 h period, increased drug release rates were observed for **ZnDiclo5** and **ZnDiclo8**, compared to **ZnDiclo6**, Fig. 3b and c. As the trends in dissolution rate do not correlate with increased linker length, it is proposed that crystal packing forces of TCP strands play a significant role in fine-tuning the TCP degradation rates. In addition, Zn^{2+} TCPs overall exhibited much slower drug release in comparison to the Mn^{2+} and Mg^{2+} analogues which demonstrated complete degradation over a 72 h period. In comparison, the Zn^{2+} TCPs released a maximum of 25% after three days and as little as just 7% in the case of **ZnDiclo6**. Overall, the release rate of Diclofenac from TCPs can be coarse-tuned and fine-tuned by (i) altering the metal ions used in TCPs, and (ii) changing the length of the bis-imidazole linker utilized, respectively.

To further investigate the drug release properties of TCPs using traditional methods,[44] buffer solutions with alternative compositions, pH, and surfactants were utilized in degradation studies. When citrate buffer (0.01 M, pH 5.5) was utilized, the release of Diclofenac from monoliths of Zn^{2+} TCPs was significantly increased in comparison to the release using phosphate buffer (0.05 M, pH 6.8). Citrate is a known metal chelator[45] and, in this case, leads to enhanced degradation of Zn-based TCPs. Alternatively, the release of Diclofenac from **MnDiclo6** and **MgDiclo6** in citrate buffer decreased marginally, still achieving complete release after 48 and 72 h, respectively (Fig. S66†). The addition of a surfactant, such as sodium dodecyl sulfate (SDS), is known to increase the hydrophilicity of the dissolution media and promotes drug dissolution.[46] The addition of 0.05% SDS to the citrate buffer resulted in all TCP monoliths completely dissolving after three days (Fig. S67†). The results with SDS give insight into how TCPs may degrade in the presence of gastrointestinal fluids if taken orally.[47] It is noted that living cells are highly sensitive to SDS and this media was not used in subsequent cytotoxicity studies.

Intrinsic dissolution rates and stimuli-responsive behavior

Although these dissolution tests provided important qualitative drug release profiles for pressed monoliths of TCPs, this methodology is not appropriate for obtaining quantitative degradation/drug release rates due to the changing surface area of the monolith during the experiment. To circumvent this deficiency, we utilized an alternative approach commonly employed to study solid-form pharmaceuticals. Degradation-based drug release rates were determined using a Woods apparatus commonly used to determine intrinsic dissolution rates (IDR) of pure solid form pharmaceuticals where the contact surface area of the material with the dissolution media is kept constant by pressing the material into a circular die before the degradation experiment.[48,49] We have not been able to find any other example in the literature in which the intrinsic dissolution rate for a series of coordination polymers containing pharmaceuticals has been reported. The IDR values from TCPs obtained in phosphate buffer 0.05 M, pH 6.8 @ 37 °C utilizing this method followed the same trends observed in the dissolution studies. However, now by keeping a constant surface area, zero-order drug release kinetics were observed with prolonged release rates over extended periods from 1 to 92 h over the duration of the experiment (Fig. 3c).

The IDR values, summarized in Table 1, compare the release of Diclofenac from TCPs with the common pharmaceutical form of the drug Sodium Diclofenac and exhibit a wide range of release rates from 958 to 0.815 – μg cm^{-2} min^{-1} (Fig. S70–S75†). To quantify how drug release rates of TCPs would change in the presence of a chemical trigger (*i.e.*, competitive metal chelators), the IDR of Zn^{2+} TCPs was determined by adding disodium EDTA to the buffer solution. When 0.05 wt% of disodium EDTA was added to the phosphate buffer solution (0.05 M, pH 6.8), there was a dramatic increase in the release of Diclofenac from the Zn^{2+} TCPs of one order in magnitude, Table 1 (Fig. S76–S81†). Furthermore, the release rate of Diclofenac from **MnDiclo6** nearly doubled from 43.7 to 76.2 μg cm^{-2} min^{-1}, whereas **MgDiclo6** only increased by 32%, from 149 to 197 μg cm^{-2} min^{-1}. With the inclusion of disodium EDTA in the IDR investigation, the TCPs exhibit an even more diverse range of release rates which can be tuned based on competitive metal chelators, such as small molecules or endogenous proteins. The ability to enhance degradation rates could even be used to trigger drug release from an implant upon ingestion of a non-toxic selective metal chelator.

Table 1 Intrinsic dissolution rates of TCPs (μg cm^{-2} min^{-1})

	Phosphate buffer 0.05 M, pH 6.8	Phosphate buffer w/0.05% Na_2EDTA
NaDiclo	958 ± 394 (ref. 52)	N/A
MgDiclo6	149 ± 4.65	197 ± 7.64
MnDiclo6	43.7 ± 1.60	76.2 ± 5.20
ZnDiclo5	2.12 ± 0.101	18.6 ± 2.35
ZnDiclo8	1.47 ± 0.0451	13.4 ± 1.23
ZnDiclo6	0.815 ± 0.0928	9.57 ± 1.96
CuDiclo6′	N/A	7.70 ± 1.09

The trends observed for the degradation rates of TCPs (*i.e.*, drug release rates) when altering the metal ion used in their construction ($Mg^{2+} < Mn^{2+} < Zn^{2+} < Cu^{2+}$) follow known trends of Lewis acidity[50] and formation constants for these metal ions.[40,51] Importantly, this level of control demonstrates the advantage degradation-based release from TCPs has in comparison to diffusion-based release from porous systems, such as organic polymers or metal–organic frameworks.[35] When TCPs are placed in an aqueous buffer media with competitive ions (*e.g.*, phosphate, citrate, or EDTA), these ions enhance the degradation at a rate which correlates with the strength and stability of the metal–ligand interactions, in this case, between the carboxylate group of the Diclofenac anion and the metal center. In addition, the degradation rate can be further fine-tuned by altering the linker's chain length. This ultimately alters how TCPs organize in the solid state (the material's overall crystal lattice energy), and potentially the accessibility competitive ions (*e.g.*, phosphate, citrate, and EDTA) have to the metal center.

Cytotoxicity of TCPs and discussion

Cytotoxicity studies of TCP materials were completed by performing an assay in which 4-[3-(4-iodophenyl)-2-(4-nitro-phenyl)-2*H*-5-tetrazolio]-1,3-benzene sulfonate (WST-1) was used to monitor cell viability.[31] TCPs were digested in 0.05 M phosphate buffer at pH 6.8, and human skin fibroblast (*NHF2*) cells were exposed to the digested solutions. The results indicated that at a concentration of 10–20 μM, the Zn^{2+} and Mg^{2+} material digests did not inhibit the formation of the formazan derivative of WST-1, indicating no apparent toxicity in comparison to the sodium salts of the pure drug forms currently used commercially (Fig. 4). In comparison, the Mn^{2+}-based TCP did exhibit a significant reduction in cellular viability at a 20 μM concentration, which was also indicated by the cells' altered morphology upon visual inspection. To reduce previously reported interference of metal ions on formazan formation[53] in the WST-1 assay, absorbance values for all TCPs were obtained in the absence of cells and subtracted from the final values as a means of normalization.[41] Furthermore, this data was supported qualitatively through microscopic imaging where reductions in cell number and condensed cell morphologies were observed following treatment with Mn^{2+}-based TCPs. Interestingly, previous work conducted by Frade *et al.* supports the notion of Mn-associated cytotoxicity in normal skin fibroblasts, compared to iron and gadolinium ionic liquids.[54]

The TCPs reported herein offer a series of unique advantages which make them highly suitable as drug release materials, including (i) tailored drug release rates which can be modified by choice of metal ion and bis-imidazole linker, resulting in intrinsic dissolution rates which span several orders of magnitude; (ii) a simple, easily scalable one-step synthetic procedure which does not require covalent modification of the target drug; (iii) high wt% of the pharmaceutical (~62–69%) within the 'matrix'; (iv) a consistent and reproducible chemical composition; and (v) stimuli-responsive behavior which demonstrates that TCPs can be triggered to release their payload under changes in pH or *via* the addition of chemical triggers, such as competitive metal chelators (*e.g.*, Na_2EDTA).

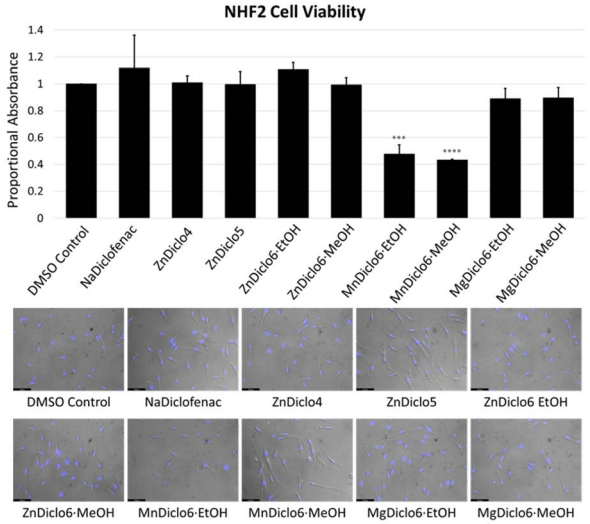

Fig. 4 Na^+, Zn^{2+}, and Mg^{2+} materials display no significant impact on NHF2 cell viability. A WST-1 assay and Hoechst nuclear stain with fluorescent microscopy were used to quantify cell viability and examine cell morphology, respectively, following 48 h treatment of NHF2 cells with the indicated materials at 20 μM. Values are expressed as a proportion of the untreated control as mean ± SD from 3 independent experiments. ***P < 0.001, ****P < 0.0001 compared to untreated control. Micrographs were taken at 200× magnification. Scale bar = 100 μm.

Perhaps the most obvious concern with TCPs as drug-release materials is their potential toxicity arising from the organic linkers and metal ions. The WST-1 cellular viability assay indicates promising initial results regarding the low toxicity of TCPs constructed from Mg^{2+} and Zn^{2+}, in comparison to the commonly used alkali metal salt of the target drug (*e.g.*, sodium Diclofenac). In addition, it is also important to note that TCPs contain a low weight percentage of metal ions ~2.7–7.7% which can easily fall below the recommended daily intake of several essential metals, such as Mg and Zn-based TCPs. To give a particular example, sodium Diclofenac is currently prescribed in 100 mg oral doses for chronic conditions, such as Rheumatoid Arthritis.[55,56] However, in extreme cases, larger doses can be prescribed, but only if the therapeutic benefit outweighs the known adverse effects. The same amount of Diclofenac released from **MgDiclo6** offers a slower release rate and only contains a small fraction of ~3 mg of the daily recommended dose of Mg^{2+} (~300–400 mg).[57] In comparison, a dose containing 100 mg of Diclofenac from **ZnDiclo6** would contain just under 11 mg of zinc, which is actually below zinc's daily recommended intake.[58,59]

Conclusions

This work has provided the foundation required to create tailor-made drug-release materials based on TCPs in which drug release rates can be primarily tuned by the strength of metal–ligand interactions, and finely tuned by altering the organic linkers used in their formation. These preliminary studies demonstrate the significant advantages of TCPs, which could be used in a variety of applications. For example, the ability to have consistent zero-order release kinetics from a drug-releasing implant is critical for drugs with a narrow therapeutic index or with short elimination half-lives.[3] Additionally, in the case of medical implants, TCPs offer a significantly higher weight % of pharmaceuticals compared to most drug release materials, such as amorphous polymer dispersions, allowing for a larger drug payload that can be administered. TCPs with very slow-release rates (>24 h), such as Zn-based TCPs, could be incorporated into post-surgical implants used to release target drugs (*i.e.*, chemotherapy agents) at the desired site of action. This could be particularly beneficial after the resection of a tumour to eradicate residual cancer cells remaining near the surgical site, akin to the currently utilized Gliadel wafer.[10] Alternatively, TCPs with release rates (<24 h), such as Mg-based TCPs, could be used to reduce the dosing requirements for orally-taken medications, allowing patients to take fewer pills, and improve patient compliance.[60] While further toxicity and *in vivo* testing of TCP materials is required these initial results demonstrate promising tunability in drug release properties. Whether drugs are taken in the form of a pill or implanted after surgery in the form of a small degradable implant, the ability to tailor drug release rates *via* TCPs could impact several different therapeutic routes of drug administration. Moreover, the use of TCPs could be extended to the fields of veterinary medicine, nutraceuticals, cosmetics, and even agrochemicals, which would benefit from extended-release applications. Work towards these goals is ongoing in our laboratory.

Experimental procedures

All reagents and solvents were purchased from commercially available sources and used without further purification. Metal salts $Cu(NO_3)_2 \cdot 1/25H_2O$, $Zn(NO_3)_2 \cdot 6H_2O$, $Mg(NO_3)_2 \cdot 6H_2O$, and $Mn(NO_3)_2 \cdot 5H_2O$, as well as ethylenediaminetetraacetic acid, were purchased from Sigma Aldrich. Imidazole, 1,5-dichloropentane, 1,6-dichlorohexane and 1,8-dichlorooctane were purchased from Oakwood Chemicals. Diclofenac and Diclofenac sodium salt were purchased from Ontario Chemicals Inc. Sodium dodecyl sulfate was purchased from Fisher. All chemicals were used without further purification. 1,1′-(1,5-pentanedidyl)bis(imidazole) (biim-5), and 1,1′-(1,6-hexanedidyl) bis(imidazole) (biim-6) and 1,1′-(1,8-octanedidyl)bis(imidazole) were successfully synthesized according to a literature procedure.[61,62]

Preparation of therapeutic coordination polymers

$Cu(Diclo)_2(biim\text{-}5)$ *CuDiclo5*. Biim-5 (0.204 g, 1.0 mmol) and Diclofenac (0.148 g, 0.5 mmol) were mixed in methanol (10 mL) at ambient temperature. A solution of $Cu(NO_3)_2 \cdot 1/2\ 5H_2O$ (0.038 g, 0.2 mmol) in methanol (1 mL) was added dropwise with stirring to the linker-Diclofenac solution. No solid was immediately formed, resulting in a clear dark blue solution. After a few minutes, crystalline material began forming. After 24 h, dark violet crystals were washed with cold methanol and dried at room temperature. Yield: 174 mg (84%), elemental

analysis found: C 54.19; H 3.98; N 9.73; $C_{39}H_{36}Cl_4CuN_6O_4$ requires: C 54.59; H 4.23; N 9.79.

Cu(Diclo)$_2$(biim-6)·(MeOH)$_2$ *CuDiclo6*. The target TCP was synthesized using the same synthetic conditions used for ***CuDiclo5***, except biim-6 was used in place of biim-5. Crystals started forming almost immediately after all components were mixed. After 24 h, pale violet crystals were washed with cold methanol and dried at room temperature. Yield: 115 mg (66%, based on the loss of MeOH, as seen in elemental analysis). Elemental analysis found: C 54.82; H 4.17; N 9.51; $C_{42}H_{46}Cl_4CuN_6O_6$ requires: C 53.88; H 4.95; N 8.98. This coordination polymer has methanol in the lattice and crystals crack in the air, partially releasing the methanol. The analytical result matches more closely with the loss of two methanol, where the chemical formula becomes $C_{40}H_{38}Cl_4CuN_6O_4$ and requires C 54.96; H 4.38; N 9.61.

Cu(Diclo)$_2$(biim-8)·(MeOH)$_2$ *CuDiclo8*. The target TCP was synthesized using the same synthetic conditions used for ***CuDiclo5***, except biim-8 was used in place of biim-5. Pale violet crystals were isolated after 24 h and washed with methanol and dried at room temperature. Yield: 193 mg (66%), Elemental analysis found: C; H; N; $C_{44}H_{50}Cl_4CuN_6O_6$ requires: C 54.81; H 5.23; N 8.72.

Zn(Diclo)$_2$(biim-5) *ZnDiclo5*. Biim-5 (0.204 g, 1.0 mmol) and Diclofenac (0.148 g, 0.5 mmol) were mixed in methanol (10 mL) at ambient temperature. A solution of $Zn(NO_3)_2\cdot 6H_2O$ (0.149 g, 0.5 mmol) in methanol (2.5 mL) was added dropwise with stirring to the linker-Diclofenac solution. No solid was immediately formed, resulting in a clear colorless solution. After a few hours, crystalline material began forming. After 48 h, colorless crystals were washed with cold methanol and dried at room temperature. Yield: 352 mg (82%), elemental analysis found: C 54.76; H 4.23; N 9.68; $C_{39}H_{36}Cl_4N_6O_4Zn$ requires: C 54.47; H 4.22; N 9.77.

Zn(Diclo)$_2$(biim-6)·(MeOH) *ZnDiclo6·MeOH*. The target TCP was synthesized using the same synthetic conditions used for ***ZnDiclo5***, except biim-6 was used in place of biim-5. After a few minutes, crystalline material began forming. After 24 h, colorless crystals were washed with cold methanol and dried at room temperature Yield: 415 mg (92%), Elemental analysis found: C 54.17; H 4.66; N 9.46; $C_{41}H_{42}Cl_4N_4O_5Zn$ requires: C 54.36; H 4.67; N 9.22.

Zn(Diclo)$_2$(biim-6)·(EtOH) *ZnDiclo6*. Synthesized the same as ***ZnDiclo6·MeOH***, except components were dissolved in ethanol instead of methanol. After a few minutes, crystalline material began forming. After 24 h, colorless crystals were washed with cold methanol and dried at room temperature. Yield: 373 mg (81%), Elemental analysis found: C 54.35; H 4.74; N 9.26; $C_{42}H_{44}Cl_4N_6O_5Zn$ requires: C 54.83; H 4.82; N 9.14.

Zn(Diclo)$_2$(biim-8) *ZnDiclo8*. Biim-8 (0.246 g, 1.0 mmol) and Diclofenac sodium salt (0.318 g, 1.0 mmol) were mixed in methanol (10 mL) at ambient temperature. A solution of $Zn(NO_3)_2\cdot 6H_2O$ (0.149 g, 0.5 mmol) in methanol (2.5 mL) was added dropwise with stirring to the linker-Diclofenac solution. No solid was immediately formed, resulting in a clear, colorless solution. After a few hours, crystalline material began forming. After 48 h, colorless crystals were washed with cold methanol and dried at room temperature. Yield: 330 mg (73%), elemental analysis found: C 55.75; H 4.50; N; 9.36 $C_{42}H_{42}Cl_4N_6O_4Zn$ requires: C 55.93; H 4.69; N 9.32.

Mg(Diclo)$_2$(biim-6)$_2$(MeOH)$_2$ *MgDiclo6·MeOH*. Synthesized the same as ***ZnDiclo6***, except $Mg(NO_3)_2\cdot 6H_2O$ was used. After 48 h, colorless crystals were washed with cold methanol and dried at room temperature. Yield 396 mg (85%), elemental analysis found: C 56.03; H 5.17; N 9.23; $C_{42}H_{46}Cl_4MgN_6O_6$ requires: C 56.24; H 5.17; N 9.37.

Mg(Diclo)$_2$(biim-6)$_2$(EtOH)$_2$ *MgDiclo6*. Synthesized the same as ***MgDiclo6·MeOH***, except components were dissolved in ethanol instead of methanol. Colorless crystalline material began forming almost immediately. After 24 h, colorless crystals were washed with cold methanol and dried at room temperature. Yield 431 mg (93%), elemental analysis found: C 56.89; H 5.35; N 8.99; $C_{44}H_{50}Cl_4MgN_6O_6$ requires: C 57.13; H 5.45; N 9.09.

Mn(Diclo)$_2$(biim-6)$_2$(MeOH)$_2$ *MnDiclo6·MeOH*. Synthesized the same as ***ZnDiclo6***, except $Mn(NO_3)_2\cdot 5H_2O$ was used. After 48 h, colorless crystals were washed with cold methanol and dried at room temperature. Yield: 432 mg (93%), elemental analysis found: C 54.40; H 5.01; N 9.00; $C_{42}H_{46}Cl_4MnN_6O_6$ requires: C 54.38; H 5.00; N 9.06.

Mn(Diclo)$_2$(biim-6)$_2$(EtOH)$_2$ *MnDiclo6*. Synthesized the same as ***MnDiclo6·MeOH***, except components were dissolved in ethanol instead of methanol. Colorless crystalline material began forming almost immediately. After 24 h, colorless crystals were washed with cold methanol and dried at room temperature. Yield: 416 mg (87%), elemental analysis found: C 55.02; H 5.07; N 8.88; $C_{44}H_{50}Cl_4MnN_6O_6$ requires: C 55.30; H 5.27; N 8.79.

Data availability

All data including experimental details supporting this article can be found in the ESI.†

Author contributions

V. N. V. conceptualized the research project with J. N. M., while J. K. and M. D. contributed to refining the research scope. V. N. V. and J. N. M. developed the experimental methodology. J. N. M. conducted the majority of the experiments with support from J. K. and M. D., while D. W. performed all toxicity testing with support from M. O. under the supervision of S. P.; V. N. V. and J. N. M. wrote the initial manuscript draft with significant input from J. K. All authors contributed to the manuscript revision, and read, and approved the submitted version. V. N. V. supervised the overall project and secured grant funding. All authors have approved the final version of the manuscript.

Conflicts of interest

V. N. V., J. N. M., J. K., and M. D. are all listed as inventors on provisional patent application No. 63/230289 (reference #26) which includes the results of this work.

Acknowledgements

V. N. V. is grateful for the awarding of an NSERC Canada Discovery Grant (RGPIN-2020-04570) in support of this research. In addition, V. N. V. and S. P. gratefully acknowledge funding for the *in vitro* toxicity provided by the University of Windsor. Additional support was provided to V. N. V. through his NSERC/PROTO Industrial Research Chair (IRC) program funded by NSERC, Proto Manufacturing Ltd., and the University of Windsor (IRCPJ 541939-18). V. N. V. and S. P. would also like to acknowledge the Canadian Foundation for Innovation, the Ontario Innovation Trust, and the University of Windsor for support of facilities within the Advanced Materials Centre for Research (AMCORe) at the University of Windsor. Several University of Windsor faculty and staff also provided constructive feedback on this article and are thanked for their valuable contributions. In addition, Maxime Le Ster is thanked for his help with the rendering of graphical images using Blender Foundation software. Ethan Douglas is also thanked for his assistance and helpful discussions.

References

1 K. E. Uhrich, S. M. Cannizzaro, R. S. Langer and K. M. Shakesheff, Polymeric systems for controlled drug release, *Chem. Rev.*, 1999, **99**(11), 3181–3198.
2 J. Gao, J. M. Karp, R. Langer and N. Joshi, The future of drug delivery, *Chem. Mater.*, 2023, **35**(2), 359–363.
3 M. L. Laracuente, H. Y. Marina and K. J. McHugh, Zero-order drug delivery: state of the art and future prospects, *J. Controlled Release*, 2020, **327**, 834–856.
4 K. I. Kaitin and K. Getz, Tufts center for the study of drug development employs broadly engaged team science to explore the challenges of pharmaceutical research and development, in *Broadly Engaged Team Science in Clinical and Translational Research*, Springer International Publishing, Cham, 2022, pp. 55–63.
5 J. Lexchin, Time to market for drugs approved in Canada between 2014 and 2018: an observational study, *BMJ Open*, 2021, **11**(7), e047557.
6 N. Kamaly, B. Yameen, J. Wu and O. C. Farokhzad, Degradable controlled-release polymers and polymeric nanoparticles: mechanisms of controlling drug release, *Chem. Rev.*, 2016, **116**(4), 2602–2663.
7 N. Shan, M. L. Perry, D. R. Weyna and M. J. Zaworotko, Impact of pharmaceutical cocrystals: the effects on drug pharmacokinetics, *Expert Opin. Drug Metab. Toxicol.*, 2014, **10**(9), 1255–1271.
8 N. K. Duggirala, M. L. Perry, Ö. Almarsson and M. J. Zaworotko, Pharmaceutical cocrystals: along the path to improved medicines, *Chem. Commun.*, 2016, **52**(4), 640–655.
9 R. Gheorghita, L. Anchidin-Norocel, R. Filip, M. Dimian and M. Covasa, Applications of biopolymers for drugs and probiotics delivery, *Polymers*, 2021, **13**(16), 2729.
10 S. A. Stewart, J. Domínguez-Robles, R. F. Donnelly and E. Larrañeta, Implantable polymeric drug delivery devices: classification, manufacture, materials, and clinical applications, *Polymers*, 2018, **10**(12), 1379.
11 V. De Leo, F. Milano, A. Agostiano and L. Catucci, Recent advancements in polymer/liposome assembly for drug delivery: from surface modifications to hybrid vesicles, *Polymers*, 2021, **13**(7), 1027.
12 S. Zhang, S. Zhang, S. Luo and D. Wu, Therapeutic agent-based infinite coordination polymer nanomedicines for tumor therapy, *Coord. Chem. Rev.*, 2021, **445**, 214059.
13 A. C. McKinlay, R. E. Morris, P. Horcajada, G. Férey, R. Gref, P. Couvreur and C. Serre, BioMOFs: metal–organic frameworks for biological and medical applications, *Angew. Chem., Int. Ed.*, 2010, **49**(36), 6260–6266.
14 R. F. Mendes, F. Figueira, J. P. Leite, L. Gales and F. A. Paz, Metal–organic frameworks: a future toolbox for biomedicine?, *Chem. Soc. Rev.*, 2020, **49**(24), 9121–9153.
15 F. C. Herbert, S. S. Abeyrathna, N. S. Abeyrathna, Y. H. Wijesundara, O. R. Brohlin, F. Carraro, H. Amenitsch, P. Falcaro, M. A. Luzuriaga, A. Durand-Silva and S. D. Diwakara, Stabilization of supramolecular membrane protein–lipid bilayer assemblies through immobilization in a crystalline exoskeleton, *Nat. Commun.*, 2021, **12**(1), 2202.
16 J. An, S. J. Geib and N. L. Rosi, Cation-triggered drug release from a porous zinc− adeninate metal− organic framework, *J. Am. Chem. Soc.*, 2009, **131**(24), 8376–8377.
17 H. Zheng, Y. Zhang, L. Liu, W. Wan, P. Guo, A. M. Nyström and X. Zou, One-pot synthesis of metal–organic frameworks with encapsulated target molecules and their applications for controlled drug delivery, *J. Am. Chem. Soc.*, 2016, **138**(3), 962–968.
18 M. W. Tibbitt, J. E. Dahlman and R. Langer, Emerging frontiers in drug delivery, *J. Am. Chem. Soc.*, 2016, **138**(3), 704–717.
19 R. Langer and N. A. Peppas, Advances in biomaterials, drug delivery, and bionanotechnology, *AIChE J.*, 2003, **49**(12), 2990–3006.
20 M. B. Giles, J. K. Hong, Y. Liu, J. Tang, T. Li, A. Beig, A. Schwendeman and S. P. Schwendeman, Efficient aqueous remote loading of peptides in poly (lactic-co-glycolic acid), *Nat. Commun.*, 2022, **13**(1), 3282.
21 W. B. Liechty, D. R. Kryscio, B. V. Slaughter and N. A. Peppas, Polymers for drug delivery systems, *Annu. Rev. Chem. Biomol. Eng.*, 2010, **1**, 149–173.
22 F. Lecomte, J. Siepmann, M. Walther, R. J. MacRae and R. Bodmeier, Blends of enteric and GIT-insoluble polymers used for film coating: physicochemical characterization and drug release patterns, *J. Controlled Release*, 2003, **89**(3), 457–471.
23 S. R. Benhabbour, M. Kovarova, C. Jones, D. J. Copeland, R. Shrivastava, M. D. Swanson, C. Sykes, P. T. Ho, M. L. Cottrell, A. Sridharan and S. M. Fix, Ultra-long-acting tunable biodegradable and removable controlled release implants for drug delivery, *Nat. Commun.*, 2019, **10**(1), 4324.
24 S. Aitipamula, R. Banerjee, A. K. Bansal, K. Biradha, M. L. Cheney, A. R. Choudhury, G. R. Desiraju, A. G. Dikundwar, R. Dubey, N. Duggirala and

P. P. Ghogale, Polymorphs, salts, and cocrystals: what's in a name?, *Cryst. Growth Des.*, 2012, **12**(5), 2147–2152.

25 G. Bolla, B. Sarma and A. K. Nangia, Crystal engineering of pharmaceutical cocrystals in the discovery and development of improved drugs, *Chem. Rev.*, 2022, **122**(13), 11514–11603.

26 J. N. Murphy, J. Kobti, M. Dao and V. N. Vukotic, *Therapeutic Coordination Polymers Containing Pharmaceuticals and Bis-Imidazole Linkers for Drug Release Applications. U.S. Patent and Trademark Office Provisional Application No. 63/230289, Filed on August 6th*, 2021.

27 M. Bartolomei, P. Bertocchi, E. Antoniella and A. Rodomonte, Physico-chemical characterisation and intrinsic dissolution studies of a new hydrate form of diclofenac sodium: comparison with anhydrous form, *J. Pharm. Biomed. Anal.*, 2006, **40**(5), 1105–1113.

28 J. Alsenz, E. Haenel, A. Anedda, P. Du Castel and G. Cirelli, Miniaturized intrinsic dissolution screening (MINDISS) assay for preformulation, *Eur. J. Pharm. Sci.*, 2016, **87**, 3–13.

29 T. Mohan, U. Ajdnik, C. Nagaraj, F. Lackner, A. Dobaj Štiglic, T. Palani, L. Amornkitbamrung, L. Gradišnik, U. Maver, R. Kargl and K. Stana Kleinschek, One-step fabrication of hollow spherical cellulose beads: application in pH-responsive therapeutic delivery, *ACS Appl. Mater. Interfaces*, 2022, **14**(3), 3726–3739.

30 H. B. Ji, S. N. Kim, S. H. Lee, B. K. Huh, B. H. Shin, C. Lee, Y. C. Cho, C. Y. Heo and Y. B. Choy, Soft implantable device with drug-diffusion channels for the controlled release of diclofenac, *J. Controlled Release*, 2020, **318**, 176–184.

31 M. Paul and P. Dastidar, Coordination Polymers Derived from Non-Steroidal Anti-Inflammatory Drugs for Cell Imaging and Drug Delivery, *Chem.–Eur. J.*, 2016, **22**(3), 988–998.

32 M. Paul, K. Sarkar, J. Deb and P. Dastidar, Hand-Ground Nanoscale ZnII-Based Coordination Polymers Derived from NSAIDs: Cell Migration Inhibition of Human Breast Cancer Cells, *Chem.–Eur. J.*, 2017, **23**(24), 5736–5747.

33 S. Bera, A. Chowdhury, K. Sarkar and P. Dastidar, Design and synthesis of znii-coordination polymers anchored with NSAIDs: metallovesicle formation and multi-drug delivery, *Chem.–Asian J.*, 2020, **15**(4), 503–510.

34 P. Biswas, K. Sarkar and P. Dastidar, Cu (II)-Metallacryptands Self-Assembled to Vesicular Aggregates Capable of Encapsulating and Transporting an Anticancer Drug Inside Cancer Cells, *Macromol. Biosci.*, 2020, **20**(6), 2000044.

35 R. S. Forgan, Reproducibility in research into metalorganic frameworks in nanomedicine, *Commun. Mater.*, 2024, **5**(46), 1–5.

36 I. Pasquali, R. Bettini and F. Giordano, Thermal behaviour of diclofenac, diclofenac sodium and sodium bicarbonate compositions, *J. Therm. Anal. Calorim.*, 2007, **90**(3), 903–907.

37 A. W. Addison, T. N. Rao, J. Reedijk, J. van Rijn and G. C. Verschoor, Synthesis, structure, and spectroscopic properties of copper (II) compounds containing nitrogen–sulphur donor ligands; the crystal and molecular structure of aqua [1, 7-bis (N-methylbenzimidazol-2′-yl)-2, 6-dithiaheptane] copper (II) perchlorate, *J. Chem. Soc., Dalton Trans.*, 1984, (7), 1349–1356.

38 S. Mallakpour, E. Nikkhoo and C. M. Hussain, Application of MOF materials as drug delivery systems for cancer therapy and dermal treatment, *Coord. Chem. Rev.*, 2022, **451**, 214262.

39 Y. Sun, L. Zheng, Y. Yang, X. Qian, T. Fu, X. Li, Z. Yang, H. Yan, C. Cui and W. Tan, Metal–organic framework nanocarriers for drug delivery in biomedical applications, *Nano-Micro Lett.*, 2020, **12**, 1–29.

40 D. A. Johnson and P. G. Nelson, Factors determining the ligand field stabilization energies of the hexaaqua 2+ complexes of the first transition series and the Irving-Williams order, *Inorg. Chem.*, 1995, **34**(22), 5666–5671.

41 M. Wątroba, W. Bednarczyk, P. K. Szewczyk, J. Kawałko, K. Mech, A. Grünewald, I. Unalan, N. Taccardi, G. Boelter, M. Banzhaf and C. Hain, In vitro cytocompatibility and antibacterial studies on biodegradable Zn alloys supplemented by a critical assessment of direct contact cytotoxicity assay, *J. Biomed. Mater. Res., Part B*, 2023, **111**(2), 241–260.

42 Note: As the TGA was run under nitrogen this gives the materials a higher thermal stability than if it was run in air.

43 D. M. Mudie, G. L. Amidon and G. E. Amidon, Physiological parameters for oral delivery and in vitro testing, *Mol. Pharmaceutics*, 2010, **7**(5), 1388–1405.

44 H. D. Williams, N. L. Trevaskis, S. A. Charman, R. M. Shanker, W. N. Charman, C. W. Pouton and C. J. Porter, Strategies to address low drug solubility in discovery and development, *Pharmacol. Rev.*, 2013, **65**(1), 315–499.

45 A. J. Francis, C. J. Dodge and J. B. Gillow, Biodegradation of metal citrate complexes and implications for toxic-metal mobility, *Nature*, 1992, **356**(6365), 140–142.

46 Y. Guo and C. C. Sun, Pharmaceutical lauryl sulfate salts: prevalence, formation rules, and formulation implications, *Mol. Pharmaceutics*, 2021, **19**(2), 432–439.

47 Z. Huang, S. Parikh and W. P. Fish, Interactions between a poorly soluble cationic drug and sodium dodecyl sulfate in dissolution medium and their impact on in vitro dissolution behavior, *Int. J. Pharm.*, 2018, **535**(1–2), 350–359.

48 C. A. Bergström, K. Box, R. Holm, W. Matthews, M. McAllister, A. Müllertz, T. Rades, K. J. Schäfer and A. Teleki, Biorelevant intrinsic dissolution profiling in early drug development: fundamental, methodological, and industrial aspects, *Eur. J. Pharm. Biopharm.*, 2019, **139**, 101–114.

49 A. Teleki, O. Nylander and C. A. Bergström, Intrinsic dissolution rate profiling of poorly water-soluble compounds in biorelevant dissolution media, *Pharmaceutics*, 2020, **12**(6), 493.

50 X. Chen and A. J. Stace, A gas phase perspective on the Lewis acidity of metal ions in aqueous solution, *Chem. Commun.*, 2012, **48**(83), 10292–10294.

51 K. J. Waldron and N. J. Robinson, How do bacterial cells ensure that metalloproteins get the correct metal?, *Nat. Rev. Microbiol.*, 2009, **7**(1), 25–35.

52 The high error for sodium diclofenac is a result of the fast dissolution time and the small sample size which quickly results in non-uniform degradation of the pressed powder in the 4 mm diameter woods apparatus.
53 E. Scarcello, A. Lambremont, R. Vanbever, P. J. Jacques and D. Lison, Mind your assays: misleading cytotoxicity with the WST-1 assay in the presence of manganese, *PLoS One*, 2020, **15**(4), e0231634.
54 R. F. Frade, S. Simeonov, A. A. Rosatella, F. Siopa and C. A. Afonso, Toxicological evaluation of magnetic ionic liquids in human cell lines, *Chemosphere*, 2013, **92**(1), 100–105.
55 B. Crowley, J. J. Hamill, S. Lyndon, J. F. McKellian, P. Williams and A. J. Miller, Controlled-release indomethacin and sustained-release diclofenac sodium in the treatment of rheumatoid arthritis: a comparative controlled clinical trial, *Curr. Med. Res. Opin.*, 1990, **12**(3), 143–150.
56 R. N. Brogden, R. C. Heel, G. E. Pakes, T. M. Speight and G. S. Avery, Diclofenac sodium: a review of its pharmacological properties and therapeutic use in rheumatic diseases and pain of varying origin, *Drugs*, 1980, **20**, 24–48.
57 R. G. Foulkes, Dietary reference intakes—calcium, phosphorus, magnesium, vitamin D, and fluoride, *Fluoride*, 1997, **30**(4), 252–257.
58 A. E. Cowan, S. Jun, J. A. Tooze, H. A. Eicher-Miller, K. W. Dodd, J. J. Gahche, P. M. Guenther, J. T. Dwyer, N. Potischman, A. Bhadra and R. L. Bailey, Total usual micronutrient intakes compared to the dietary reference intakes among US adults by food security status, *Nutrients*, 2019, **12**(1), 38.
59 R. S. Jakka, A. Mahendranath, P. Srikrishnarka, A. Anil Kumar, M. R. Islam, S. Mukherjee, L. Philip and T. Pradeep, Geologically inspired monoliths for sustainable release of essential minerals into drinking water, *ACS Sustainable Chem. Eng.*, 2019, **7**(13), 11735–11744.
60 K. S. Ingersoll and J. Cohen, The impact of medication regimen factors on adherence to chronic treatment: a review of literature, *J. Behav. Med.*, 2008, **31**, 213–224.
61 T. Fu, S. Smith, M. Camarasa-Gómez, X. Yu, J. Xue, C. Nuckolls, F. Evers, L. Venkataraman and S. Wei, Enhanced coupling through π-stacking in imidazole-based molecular junctions, *Chem. Sci.*, 2019, **10**(43), 9998–10002.
62 S. Wang, L. Ding, J. Fan, Z. Wang and Y. Fang, Bispyrene/surfactant-assembly-based fluorescent sensor array for discriminating lanthanide ions in aqueous solution, *ACS Appl. Mater. Interfaces*, 2014, **6**(18), 16156–16165.